J Paleolimnol (2012) 48:147–158
DOI 10.1007/s10933-012-9602-9

ORIGINAL PAPER

A sedimentary and geochemical record of water-level changes from Rantin Lake, Yukon, Canada

D. P. Pompeani · B. A. Steinman · M. B. Abbott

Received: 15 September 2011 / Accepted: 14 March 2012 / Published online: 24 April 2012

Abstract A multi-proxy analysis of two sediment cores from Rantin Lake are used to reconstruct past lake-level changes and to make inferences about millennial-scale variations in precipitation/evaporation (P/E) balance in the southern Yukon, Canada between 10,900 and 3,100 cal yr BP. Analyses of calcium carbonate and organic matter concentration, magnetic susceptibility, titanium content, dry bulk density, and macrofossils are used to reconstruct water-level changes. The development of sand layers and deformed sediments at the deep-water core site (i.e. Core A-06) prior to ~10,900 cal yr BP suggest that lake level was lower at this time. Fine-grained organic sediment deposited from 10,600 to 9,500 cal yr BP indicates a rise in lake level. The formation of an unconformity at the shallow cores site (Core C-06) and the deposition of shallow-water calcium carbonate-rich facies at the Core A-06 site between ~9,500 and ~8,500 cal yr BP suggest lower lake levels at this time. Shallow-water facies gradually transition into a sand layer that likely represents shoreline reworking during an extreme lowstand that occurred at ~8,400 cal yr BP. Following this low water level, fine-grained organic-rich sediment formed by ~8,200 cal yr BP, suggesting deeper water conditions at core site A-06. Calcium carbonate concentrations are relatively low in sediment deposited from ~6,300 to 3,100 cal yr BP in Core A-06, indicating that lake level was comparatively higher during the middle and late Holocene. In general, results from this study suggest that the early Holocene was characterized by high P/E from ~10,500 to 9,500 cal yr BP, low P/E from ~9,500 to 8,400 cal yr BP, and return to higher P/E from ~8,200 to 3,100 cal yr BP.

Keywords Climate · Holocene · Drought · Lake sediment · Calcium carbonate · Pollen

This is one of 18 papers published in a special issue edited by Darrell Kaufman, and dedicated to reconstructing Holocene climate and environmental change from Arctic lake sediments.

D. P. Pompeani (✉) · B. A. Steinman · M. B. Abbott
Department of Geology and Planetary Science, University of Pittsburgh, Pittsburgh, PA 15260, USA
e-mail: dpp7@pitt.edu

Introduction

The geochemical composition of lake sediment is strongly influenced by water depth. Within surficially closed-basin lakes that produce authigenic calcium carbonate ($CaCO_3$) minerals, differences in CO_2, sunlight intensity, salinity and temperature in the water column can lead to large, predictable variations in sediment composition between shallow and deep water locations (Teller and Last 1990). As lake level varies, the depositional environment of a lakebed changes such that distinctive shallow (or littoral) water facies can form in locations previously characterized by deep water, and vice versa. For example, water-level changes can alter the physical and bio/geochemical setting of the core site, which can drive variations in the flux of carbonate, organic matter and mineral matter to the sediments (Dean 2006). Sedimentological changes can therefore provide information about millennial-scale variations in lake level resulting from changes in the regional balance between precipitation and evaporation (P/E) (Abbott et al. 2000; Anderson et al. 2005). The interplay between biological and physiochemical processes complicates lake-level interpretations of sedimentary carbonate records, making it necessary to characterize and constrain lake-level variability at multiple settings within a lake.

Here we characterize sediment facies recovered from the shallow and deep areas of Rantin Lake (60.0296°N, 129.0323°W, 720 m asl) to reconstruct past water-level changes. Cores recovered from the modern littoral (Core C-06, 1.0 m water depth) and benthic zones (Core A-06, 9.6 m water depth) are used to characterize the physical and bio/geochemical composition of the facies associated with different water depths. To reconstruct past lake levels, we assess radiocarbon-dated unconformities and sedimentological changes (e.g. calcium carbonate concentrations). We then compare the lake-level record to a previously developed pollen record from Rantin Lake (referred to as "Hail Lake" by Cwynar and Spear 1995) to investigate the association between paleovegetation changes and shifts in regional P/E. Finally, we discuss the Rantin Lake water-level record in the context of other lake-level reconstructions from the region.

Setting

Rantin Lake is located in the boreal forest of southeastern Yukon, Canada in a low-relief valley of glaciofluvial origin, north of a small western tributary stream of the Upper Liard River (Doherty et al. 1994). The watershed is large and hummocky with minimal surficial drainage, containing a series of small lakes that are hydrologically connected through groundwater flow (Fig. 1). The substrate is characterized by scattered permafrost atop fluvial gravels and sands derived from reworked glacial outwash (Doherty et al. 1994; Lipovsky et al. 2005). Black spruce (*Picea mariana*) and white spruce (*Picea glauca*) predominate in the regional forest with a notable presence of lodgepole pine (*Pinus contorta*), white birch (*Betula papyrifera*), and aspen (*Populus balsamifera*) (Cwynar and Spear 1995). Rantin Lake is surficially closed, has a small surface area (~0.08 km^2) and a bowl-shaped basin with a maximum depth of 11 m. *Chara* algae grow in the shallow water carbonate platforms along the perimeter of the lake. Field observations indicate the presence of *Chara* in shallow water, suggesting that the lighter color of shallow water sediments is caused by the presence of biomediated calcium carbonate (Kelts and Hsü 1978; Yu et al. 2008).

The regional climate is sub-arctic and characterized by warm, wet summers and dry, cold winters. Climate data from nearby Watson Lake airport (60.12°N, 128.82°W; 687 m asl; 1971–2000 AD) indicate an average annual temperature of −2.9 °C with an average annual precipitation amount of 404 mm. Summer temperature averages 13.6 °C (Fig. 1). Approximately 196 mm (or 49 %) of the total annual precipitation falls from May to August (Environment Canada 2010). Observations suggest that the strength and position of the Aleutian Low (AL) influence the trajectory of regional air masses and the intensity of precipitation (Bryson and Hare 1974; Mock et al. 1998; Wahl et al. 1987). During a positive or 'warm phase' of the Pacific Decadal Oscillation (PDO) the AL is strengthened and/or located farther to the east, leading to a stronger meridional component to the Pacific westerlies, an increase in precipitation along the Alaskan coastal mountain barrier, and potentially reduced precipitation amounts in the interior rain shadow (Streten 1974; Wahl et al. 1987). During 'cool phase' PDO conditions the AL is weakened and/or more westward, producing wetter conditions across the interior regions of the Yukon.

Materials and methods

Fieldwork

During July 2006, three sediment cores were collected from Rantin Lake. Core A-06 was collected using a square-rod piston corer (Wright et al. 1984) in 9.6 m of water (which is well below the thermocline) and consists of four overlapping drives penetrating 3.6 m into the sediment (Fig. 2). Core B-06 was collected adjacent to the A-06 site using an Aquatic Research hammer core. Mixed high- and low-density layers

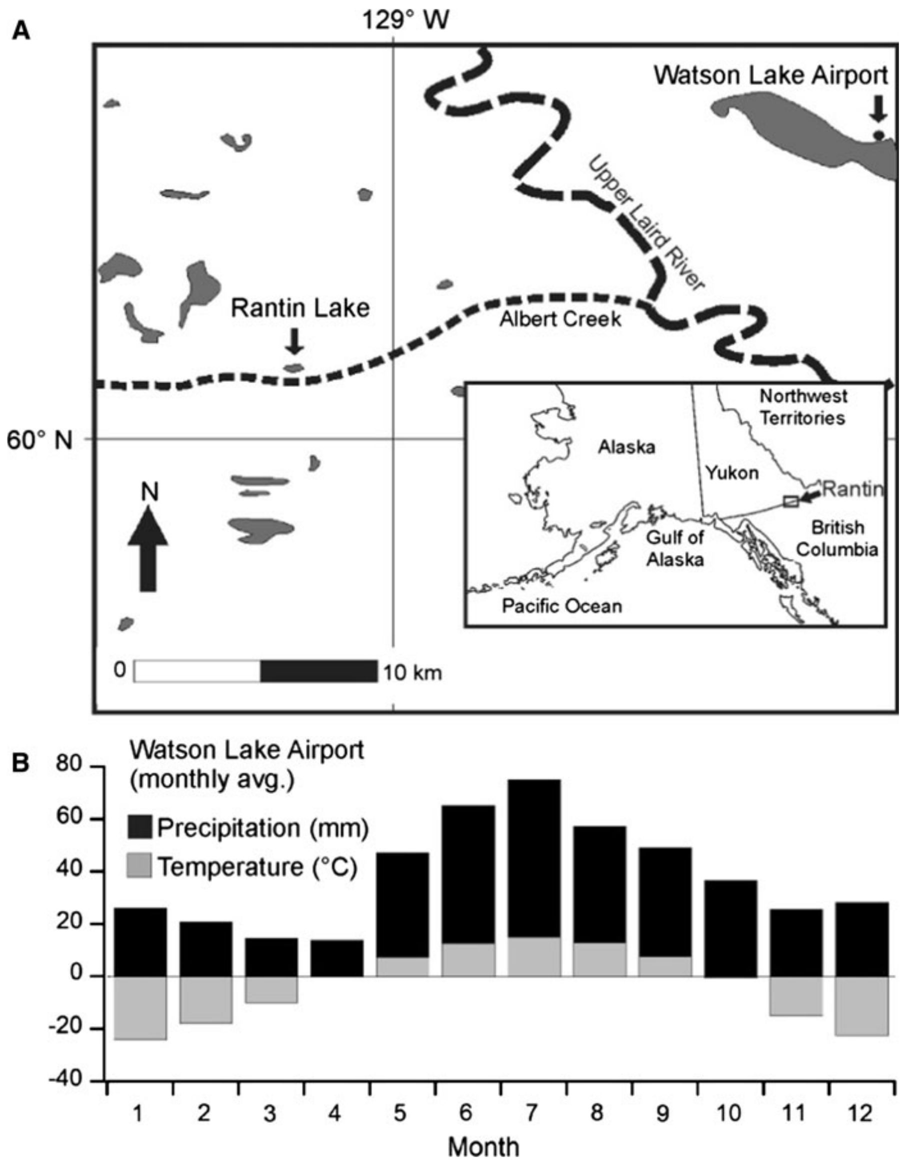

Fig. 1 **a** Rantin Lake location map. The lake is situated above a small tributary of the Upper Laird River. **b** Average monthly temperature and precipitation from nearby Watson Lake Airport (Environment Canada 2010)

in the upper section of Core B-06 resulted in a poorly preserved sediment–water interface and what appeared to be multicentimeter-thick gaps in the sediment sequence where denser sediment layers blocked the leading end of the core tube and impeded the recovery of lower-density layers. Therefore Core B-06 was not used for laboratory analyses. Core C-06 was recovered using a square-rode piston corer in 1.0 m of water (which was well above the thermocline), and consists of four overlapping drives that penetrate 3.40 m into the sediment. Individual core drives were double wrapped in polyvinyl plastic, sealed in schedule 40 PVC tubing and transported to the Department of Geology and Planetary Science at the University of Pittsburgh. Physical water parameters were measured prior to coring at each site using a Hach® Hydrolab water quality sonde equipped with sensors for measuring lake water temperature, specific conductivity, dissolved oxygen, and pH.

Sediment core analysis

Sediment cores were split, digitally photographed, and characterized by color, sedimentary structure, and macrofossil content. Individual drives for Cores A-06 and C-06 were stratigraphically correlated using

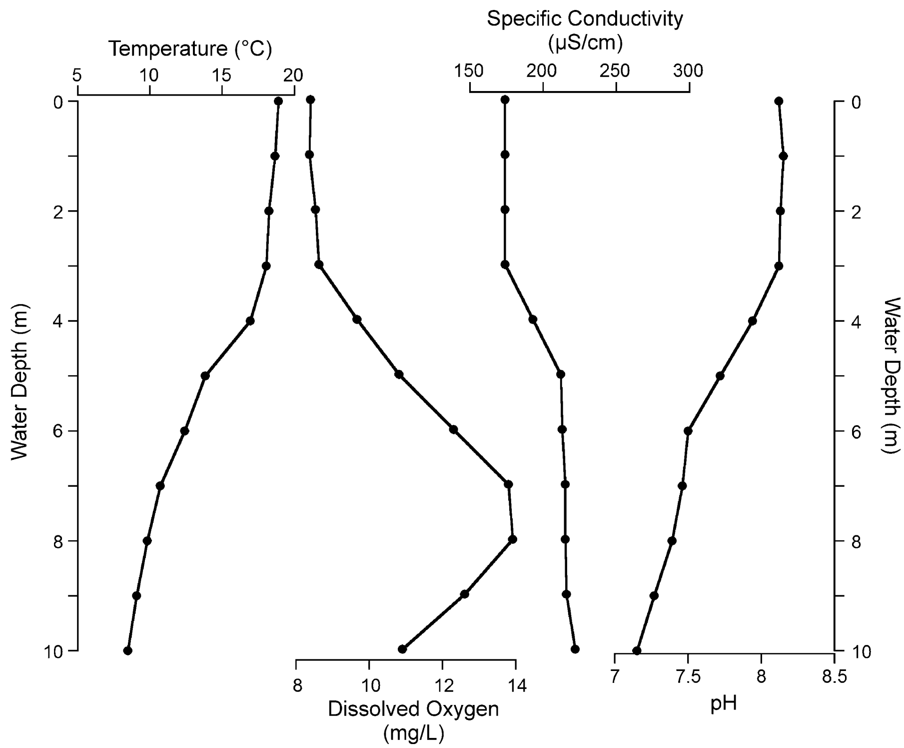

Fig. 2 Limnological measurements of the Rantin Lake water column, July 2006, showing thermal and chemical stratification at ~4 m water depth

distinct facies to determine a composite depth scale. The upper sediment from Core B-06 was considered to be unreliable because of disturbances during coring so we focused on the sections below 65 cm where Core A-06 sediments were well preserved. Core A-06 was sub-sampled continuously at 1 cm resolution, and Core C-06 was sub-sampled at 3–5 cm resolution for bulk density and loss-on-ignition (LOI) analyses. The 1 cm^3 subsamples were weighed wet, and then dried for 24 h at 60 °C to estimate dry density (g/cm^3). Organic matter, calcium carbonate, and residual mineral matter content as a weight percentage were measured by LOI at 550 °C for 4 h and 1,000 °C for 2 h (Dean 1974; Heiri et al. 2001). Titanium (Ti) concentrations of Core C-06 were measured using an ITRAX® scanning X-ray fluorescence (XRF) instrument (0.4 cm resolution) at the University of Minnesota-Duluth Large Lakes Observatory (Croudace et al. 2006). XRF values are presented in counts per second (CPS). Magnetic susceptibility was measured at 0.2 cm intervals at room temperature using a Tamiscan high-resolution surface-scanning sensor connected to a Bartington susceptibility meter. The mineralogy of Core A-06 was investigated by X-ray diffraction (XRD) using a Philips PW3710 X'Pert® X-ray Diffractometer at the University of Pittsburgh Department of Engineering. Samples for XRD were pretreated using 35 % H_2O_2 for 12 h at room temperature to remove organic matter. The sediments were then rinsed with deionized water, frozen, dehydrated and homogenized prior to being mounted on a glass slide for analysis. Four samples from Core A-06 were analyzed to characterize the general mineralogical composition of the sediment at 79.0, 199.5, 244.0, and 291.5 cm depth.

Geochronology

Bulk sediment samples were disaggregated in 7 % H_2O_2 for ~12 h and sieved at 63 μm to isolate terrestrial macrofossils which were handpicked using a small brush under a binocular microscope for radiocarbon measurements. Samples were pretreated using an acid–base-acid wash and rinsed to pH neutrality with deionized water (Abbott and Strafford 1996). Analyses were conducted at the W.M. Keck Carbon Cycle Accelerator Mass Spectrometry Laboratory at the University of California, Irvine (UCI). A total of 25 radiocarbon ages were obtained (Table 1). All radiocarbon ages were calibrated with Calib 6.0.1

Table 1 Radiocarbon data with calibrated ages

UCIAMS #	Core	Drive	Depth below lake floor (cm)	Material	^{14}C Age (yr BP)	Error	Median calibrated age (yr BP)	$+2\sigma$ Error upper	-2σ Error lower
75944	A-06	D1	73.75	Seeds	3,420	45	3,675*	3,830	3,570
75945	A-06	D1	77.75	Charcoal	2,940	110	3,105	3,370	2,810
71428	A-06	D2	150.25	Charcoal	4,515	25	5,155	5,300	5,050
58723	A-06	D2	160.50	Wood	5,125	25	5,895	5,930	5,755
75946	A-06	D2	190.50	Charcoal	7,120	100	7,945	8,165	7,740
71429	A-06	D3	208.50	Wood	7,960	160	8,830	9,255	8,430
76105	A-06	D3	214.50	Wood	8,910	230	9,990*	9,490	10,570
76106	A-06	D3	219.50	Seeds	9,060	30	10,225*	10,245	10,194
71430	A-06	D3	232.50	Charcoal	8,450	60	9,475	9,540	9,310
71431	A-06	D3	239.25	Seed	8,575	35	9,540	9,595	9,490
58724	A-06	D3	284.00	Wood	9,615	35	10,935	11,165	10,780
76107	A-06	D4	291.75	Wood	42,600	1,400	46,005*	49,105	43,835
71432	A-06	D4	334.50	Wood	49,500	1,600	n/a*	n/a	n/a
71433	A-06	D4	354.50	Wood	9,030	200	10,140*	10,650	9,555
58746	A-06	D4	365.00	Wood	43,400	3,000	46,585*	50,000	42,805
76109	C-06	D1	9.00	Charcoal	6,375	20	7,300*	7,415	7,260
76110	C-06	D1	26.5	Charcoal	5,715	30	6,500	6,630	6,410
76111	C-06	D1	54.5	Wood	5,940	20	6,765	6,845	6,680
76112	C-06	D1	67.00	Wood	6,145	20	7,060	7,155	6,965
76113	C-06	D2	87.20	Wood	6,130	20	7,010	7,155	6,945
76114	C-06	D2	103.80	Wood	6,210	25	7,095	7,240	7,010
76115	C-06	D3	161.00	Wood	6,490	25	7,410	7,460	7,325
76116	C-06	D3	185.00	Wood	7,275	35	8,095	8,170	8,015
76117	C-06	D3	212.00	Charcoal	7,330	70	8,135	8,320	8,005
76118	C-06	D4	284.20	Wood	9,260	25	10,450	10,550	10,300

Calibrated age is the median of the probability density distribution

*Date omitted from the age model

using the INTCAL09 dataset (Stuiver et al. 1998, 2010).

Results[1]

Limnological measurements

The water column was stratified, with a thermocline and chemocline depth of 4 m in July, 2006. The epilimnion had an average pH of 8.1 and average dissolved oxygen concentration of 8 mg/l. The pH of the hypolimnion averaged 7.3 with a dissolved oxygen concentration of 12 mg/l. Chemical weathering of calcareous bedrock and till in the watershed is the most likely source of the dissolved inorganic carbon (DIC) and Ca^{2+} ions, resulting in alkaline lake water with a conductivity of 174–220 µS/cm (Fig. 2).

Age model

We applied a linear interpolation age-model to Core A-06 using eight calibrated radiocarbon age distributions to generate 95 % confidence intervals with the CLAM software for R (Fig. 3) (Blaauw 2010). We feel that the linear interpolation age model is most reliable when significant lake-level changes occur. This is the

[1] All of the data from Rantin Lake presented in this study are available on-line through the World Data Center for Paleoclimatology (http://www.ncdc.noaa.gov/paleo/pubs/jopl2012arctic/jopl2012arctic.html).

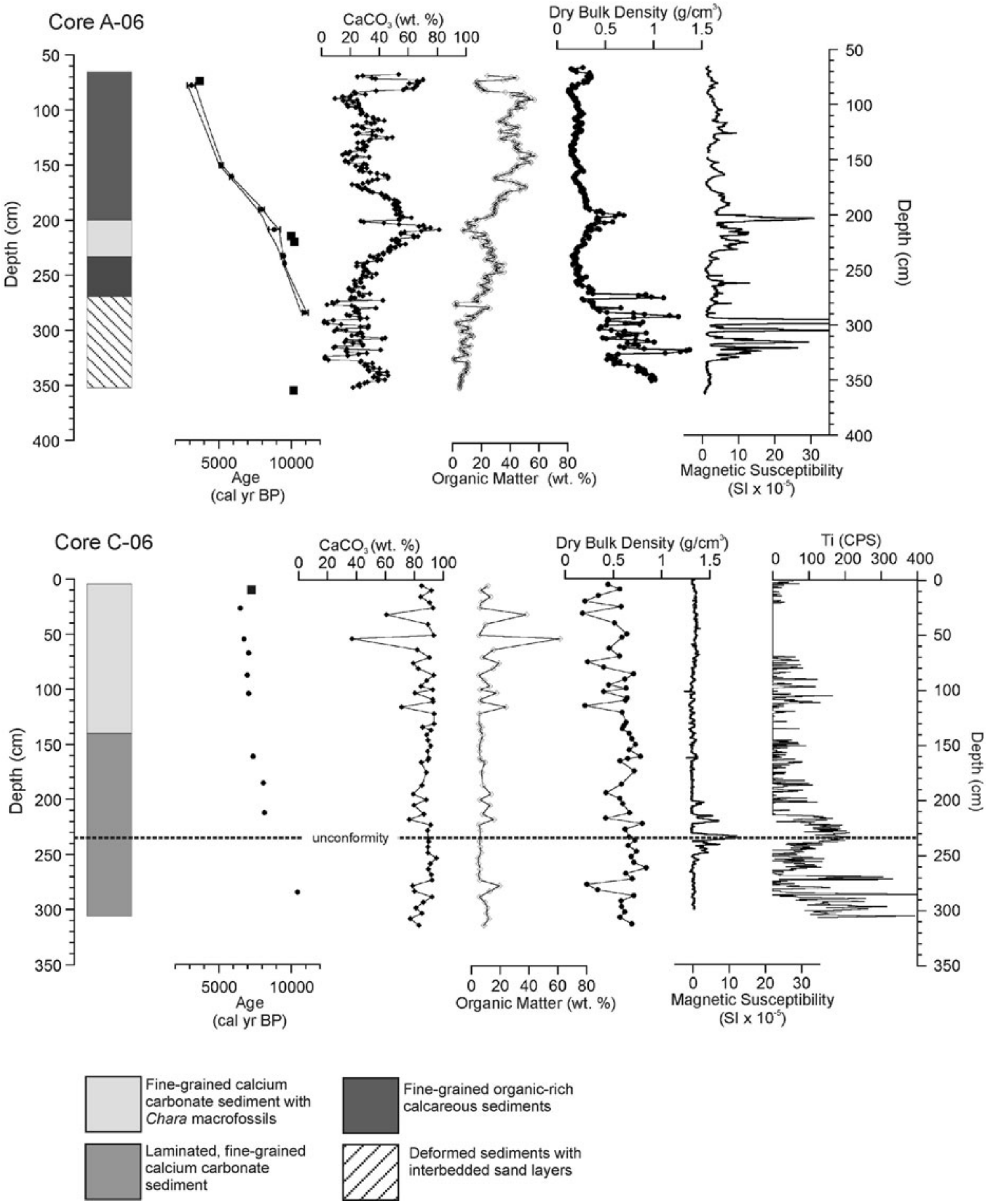

Fig. 3 Core A-06 calcium-carbonate content, organic-matter content, magnetic susceptibility, and dry bulk density (from loss-on-ignition) compared with a generalized stratigraphic column and linear interpolation age model generated using CLAM software for R (95 % confidence intervals shown). Core C-06 calcium-carbonate content, organic-matter content, Ti, and magnetic susceptibility, with a stratigraphic column and radiocarbon dates. Unconformities and substantial reworking of organic material in the upper part of the core prevents the establishment of a reliable age model

same approach used at Birch Lake (Abbott et al. 2000) and Marcella Lake (Anderson et al. 2005), which are in similar settings. Samples were chosen for radiocarbon dating above and below facies contacts wherever reliable material was isolated. Seven samples were excluded because they had older ages that imply reworking and/or contamination. Sample UCIAMS-71433, for example, was extremely small and had an exceptionally young age for its stratigraphic position (9,030 ± 200 ^{14}C years), indicating potential contamination with modern carbon during the graphitizing process. Wood fragments isolated from sediments between 290 and 365 cm were omitted (UCIAMS-76107, 71432, and 58746) from the age model because of the anomalously old ages (42,000–50,000 ^{14}C year BP). Wood preserved in this section was likely reworked during lowstand events or remobilized from melting permafrost during the early Holocene. Core A-06 LOI was continuously sub-sampled at 1 cm intervals for a temporal resolution average of 38 ± 2 years/sample. Ten radiocarbon measurements were obtained from Core C-06, with nine of the ten dates in chronological order relative to depth in the sediment. All radiocarbon age estimates are hereafter reported as calendar years before 1950 AD (cal yr BP).

Core A-06

The basal section of the core (from 357 to 245 cm) is characterized by high mineral-matter content (49–97 % by weight), high magnetic susceptibility (20–50 SI × 10^{-5}) and low organic-matter concentrations (0–29 % by weight). Calcium carbonate content is low and ranges from 10 to 38 % by weight, with higher values coincident with fine millimeter-scale laminations (Fig. 3). Sediments from 357 to 334 cm consist of deformed laminations located below a 4 cm layer of quartz sand (334–330 cm). Bands of dark mineral-rich sediment composed of detrital labradorite and andesine (indicated by XRD) are located within the deformed laminations (i.e. from 330 to 300 cm). Fine-grained mineral-rich sediment marks the transition at 300 cm to fine calcareous laminations that are overlain by a 3-cm-thick layer of quartz sand (from 280 to 277 cm). Fine horizontal laminations occur again between 277 and 265 cm. At 260 cm, laminations dip and become fine grained, coinciding with a gradual increase in organic-matter content from 10 to 30 % by weight. Between 260 and 250 cm the sediment is fine-grained, organic-rich, and calcareous, with a red color consistent with iron oxidation.

The sediments from 245 to 197 cm are have higher calcium-carbonate concentrations (25–85 %) and lower organic-matter content (7–29 %). The calcium-carbonate-rich sediment within this interval transitions from brown to white and contains abundant *Chara* macrofossils. Calcium carbonate values are high between 245 and 215 cm, where a ~5-cm-thick layer of *Chara*-rich calcium carbonate sediment is present. Above this section, magnetic susceptibility values increase from ~10 to 30 SI × 10^{-5} (between 210 and 205 cm), coincident with higher concentrations of residual mineral matter composed of detrital quartz and muscovite sands. A transition to massive organic-rich sediment occurs above this interval (at ~205 cm), along with an increase in carbonate content to values of 68 % within a section of fine laminations of authigenic calcium carbonate and organic matter at ~200 cm.

The upper section of Core A-06 from 197 to 67 cm is massively layered and has low magnetic susceptibility values (<5 SI × 10^{-5}). Organic-matter concentrations increase upward between 197 and 147 cm. Correspondingly, carbonate concentrations decline from 68 % at 197 cm to a low of 8 % at 147 cm. Between 147 and 90 cm, calcium-carbonate content ranges from 8 to 30 %, with organic-matter concentrations varying between 35 and 57 %. At a depth of 80 cm, an abrupt increase in calcium-carbonate content coincides with fine-grained millimeter-scale laminations that are white to brown. XRD analysis indicates the calcium carbonate is composed primarily of the calcite. At 72 cm, there is a 5 cm interval of massive calcareous organic-rich sediments.

Core C-06

The basal section (319–234 cm) of Core C-06 consists of fine-grained laminated sediment composed of 80–90 % calcium carbonate with intermittent of *Chara* macrofossils and little residual mineral matter (<3 % by weight) (Fig. 3). Magnetic susceptibility is low at the base (0–1 SI × 10^{-5}) while Ti is relatively high (~300 CPS). Titanium declines by 280 cm reaching a minimum of 0–100 CPS by 260 cm. Between 240 and 230 cm, magnetic susceptibility and Ti both peak within a layer that appears to be an erosional surface/unconformity. Above the erosional surface, magnetic susceptibility values decrease from a high of 12 SI × 10^{-5} and remain variable between 230 and 200 cm. Similarly, Ti decreases from a high of 200 CPS just above the unconformity (between 240 and 230 cm) and abruptly decreases to 0 CPS at depth of 210 cm. Magnetic susceptibility decreases to 0–2 SI × 10^{-5} between 230 and 200 cm. Sediments deposited during this period contain low Ti (<100 CPS) and consist of fine-grained calcium carbonate with *Chara* macrofossils layers that are indicated by higher (>20 %) organic-matter concentrations. The data were not plotted on an age model in this case because the period represented by continuous sedimentation was not long enough to justify a separate figure.

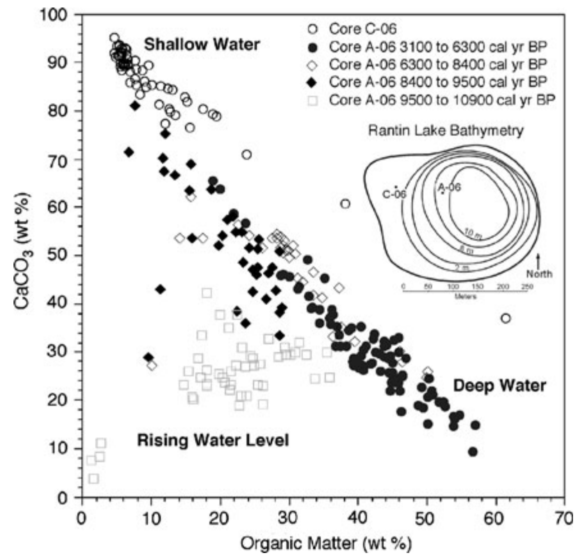

Fig. 4 Scatterplot of calcium-carbonate versus organic-matter concentrations from Cores A-06 and C-06. Shallow-water sediments are have high calcium carbonate ($CaCO_3$) concentrations (e.g. Core C-06). This contrasts with deeper-water facies, which contain lower concentrations of calcium carbonate and higher organic-matter concentrations (e.g. Core A-06). Following this conceptual model, we interpret long-term changes in calcium-carbonate concentrations within Core A-06 as a function of lake level. Inset is a bathymetric map of Rantin Lake showing cores sites A-06 in 9.6 m water depth and C-06 in 1.0 m of water

Discussion

Carbonate precipitation processes in freshwater lakes

In alkaline lakes, Ca^{2+} can react with carbonate ions to form authigenic carbonate minerals in the water column, as a result of biomediation (Kelts and Hsü 1978; Leng and Marshall 2004; Thompson et al. 1997) and/or physiochemical effects, such as temperature variations (Benson et al. 1996; Sanford and Wood 1991; Teller and Last 1990). Variability in lake-water Ca^{2+} concentration is influenced by groundwater input in surficially closed lakes. For example, authigenic calcium carbonate production in Ca^{2+} limited systems can be controlled by aquifer recharge to the groundwater supplying the lake, and is therefore closely related to P/E balance (Shapley et al. 2005).

The effects of solute concentration and temperature variations on the production of calcium carbonate at millennial timescales within Rantin Lake are not entirely understood, in part because of limited water chemistry and modern calibration data. Scatterplot analyses of calcium carbonate and organic-matter content in Rantin Lake sediment demonstrate that water depth is the primary control on sedimentary carbonate concentration at different core sites (Fig. 4). In closed-basin lakes, such as Rantin Lake, calcium carbonate production in shallow water is mediated by *Chara* photosynthesis and is relatively uninfluenced by terrigenous mineral matter input. At Rantin Lake *Chara* is ubiquitous, suggesting that biomediated calcium carbonate forms throughout the basin. However, differences in deep and shallow water temperature, light intensity, and chemistry affect the rate of photosynthetically induced carbonate production and subsequent preservation. Consequently, sediment carbonate concentrations at Rantin Lake are inversely related to water depth, an observation that has considerable implications for paleolimnological interpretations.

Lake-level reconstruction from two core sites

The complex and dynamic interplay between biological and physiochemical processes at Rantin Lake necessitates the use of at least two cores from different depths to study lake-level changes through time. Specifically, we compared lake-level reconstructions based on facies changes in the deep-water core (A-06) with the shallow water reconstruction (Core C-06) to provide a robust interpretation of lake-level change. We used unconformities, radiocarbon date reversals, and sedimentological changes resulting from basin-scale processes to reconstruct water-level variations.

It was not possible to date the basal sections of Cores A-06 and C-06 because of unreliable radiocarbon ages, several of which exceed 40,000 ^{14}C yr BP. Ancient radiocarbon ages, along with deformed sediments, imply a period of low lake levels and extensive sediment reworking. Core A-06 contains the oldest reliable date, 10,940 cal yr BP (Fig. 3). During this period, fine laminations formed at the Core A-06 location indicating relatively high water levels. A 3 cm layer of quartz sand deposited at the Core A-06 site at 10,700 cal yr BP indicates shoreline reworking and suggests that lake level dropped quickly and remained low (Fig. 5). Fine-grained sediment deposited at the Core A-06 location at 10,500 cal yr BP suggests a rise in lake-level. This indication is supported by the corresponding deposition of fine-grained calcium carbonate sediment with an age of 10,450 cal yr BP at the Core C-06 site. Collectively, evidence from the two core locations indicates lake levels had risen by the early Holocene.

Higher carbonate concentrations in Core A-06 sediment after 9,500 cal yr BP indicates declining lake levels. The presence of *Chara*, white coloration, and high carbonate concentrations in sediment from 8,800 cal yr BP suggests that littoral conditions prevailed at the Core A-06 location (Fig. 4). This inference is supported by radiocarbon reversals (UCI-AMS # 76105, 76106), which suggest low water levels and shoreline reworking. Further, high Ti concentrations and an abrupt rise in magnetic susceptibility in Core C-06 between 10,450 and 8,140 cal yr BP (230–240 cm) correspond with a distinct erosional surface. This unconformity indicates that water levels were below the Core C-06 location. Higher detrital mineral concentrations in Core A-06 at ~8,400 cal yr BP indicate the development of a shoreline near the core site. This interval represents the lowest water levels of the dated record. Above this, a transition into laminated carbonate-rich sediments occurs, implying a rise in water level shortly after 8,400 cal yr BP.

The transition to fine-grained facies with low carbonate concentrations in sediments from 8,200 cal yr BP in Core A-06 suggests a substantial lake-level increase at this time. This rise in lake level is concomitant with the decline in Ti and deposition of fine-grained sediment at core site C-06 by approximately 8,140 cal yr BP. A

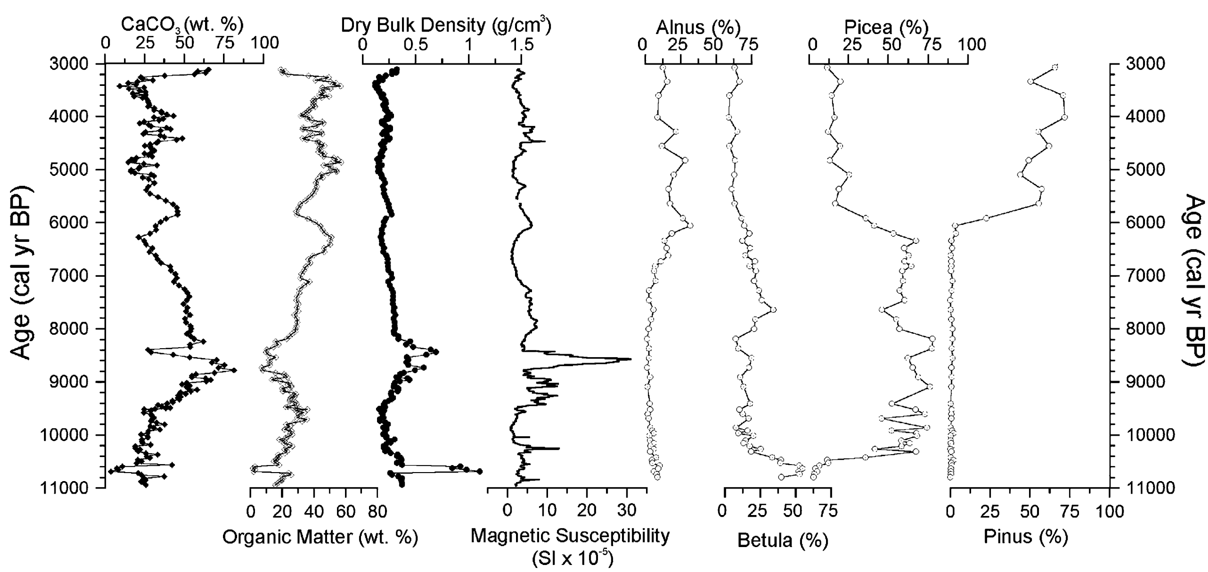

Fig. 5 The multi-proxy record of Core A-06 compared with the pollen record of Cwynar and Spear (1995). Reconstructions from Rantin Lake indicate a period of higher lake levels from ~10,500 to ~9,500 cal yr BP during a transition to higher P/E in the early Holocene. After ~9,500 cal yr BP, lake levels decreased and littoral and shoreline sediments formed in the deep basin until ~8,400 cal yr BP. Following this lowstand, lake levels rose until ~6,300 cal yr BP. Afterwards, lake levels remained variable but comparatively higher than during the early Holocene, with a trend toward lower lake levels by the end of the sediment record at ~3,100 cal yr BP. Stratigraphic changes coincide with vegetation change inferred from pollen, suggesting P/E is a major driver during these shifts

sustained decrease in calcium-carbonate concentrations in Core A-06 from ~8,100 to ~6,300 cal yr BP suggests that lake level rose and remained high. This period corresponds with the rapid accumulation of biomediated calcium carbonate sediment and subsequent reduction of accommodation space at the Core C-06 location, where little to no sediment accumulated after approximately 7,000 and 6,500 cal yr BP. Low calcium-carbonate concentrations in Core A-06 sediment from ~6,300 to 3,500 cal yr BP suggest a sustained period of high lake level during the middle Holocene. However, a long-term increasing trend in carbonate concentrations at the Core A-06 site following the minima (at ~6,300 cal yr BP) suggests that lake levels, although generally higher, slowly decreased throughout the mid-Holocene until the end of the record at 3,100 cal yr BP.

Regional climate comparison

Deformed layering in the lowermost sections of Core A-06 suggests that water levels and P/E were lower during the early Holocene. This assertion is consistent with evidence provided by Abbott et al. (2000) for multiple lowstands from ~14,000 to 10,000 cal yr BP at Birch Lake in south-central Alaska (Fig. 6). Fine-grained sediment deposited at Core A-06 by 10,900 cal yr BP suggests a transition to higher lake levels and P/E values. Comparison with a previously published pollen record from the same lake (Cwynar and Spear 1995) indicates that *Betula* predominated in forests in the area by ~10,800 cal yr BP (Fig. 5), prior to the expansion of *Picea* by ~10,400 cal yr BP. Further, decreased water levels identified at Marcella Lake in the Yukon by Anderson et al. (2005) following ~9,500 cal yr BP are consistent with Rantin Lake data, which suggest that low lake levels occured between ~9,500 and 8,400 cal yr BP.

The increase in lake level from ~8,200 to 6,300 cal yr BP likely resulted from the intensified transport of moisture to the interior Yukon region, possibly indicating a transition to more 'cool phase' PDO conditions in the North Pacific. A notable increase in *Alnus* pollen occurs in sediment deposited between ~6,800 to 6,100 cal yr BP, supporting the hypothesized middle Holocene transition to greater P/E. Around ~6,000 cal yr BP, *Pinus* rapidly migrated into the region and replaced *Picea,* which subsequently declined from ~6,000 to 5,700 cal yr BP (Cwynar and Spear 1995). A rise in carbonate concentrations within Core A-06 by ~3,100 cal yr BP suggests that P/E values were lower by the late Holocene, which is supported by the reduction in *Alnus* pollen in sediment by

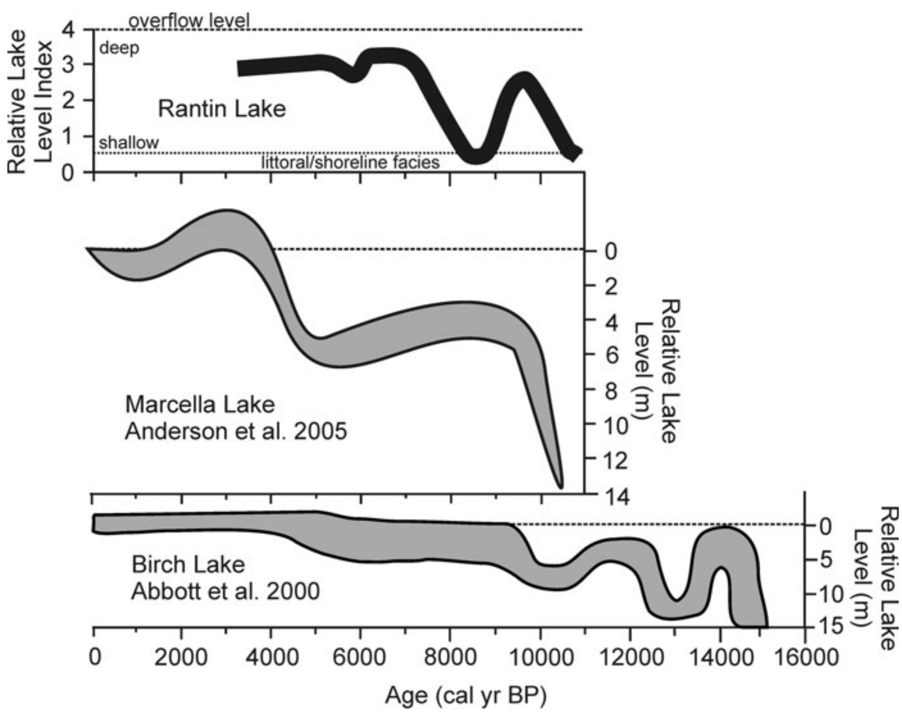

Fig. 6 Relative lake-level changes (indexed) at Rantin Lake (this study) compared with water-level reconstructions from Birch Lake (Abbott et al. 2000) and Marcella Lake (Anderson et al. 2005). The lake-level index (unitless) is based on a qualitative interpretation of the Core A-06 and Core C-06 sediment records and represents a likely lake-level change scenario

~4,000 cal yr BP (Cwynar and Spear 1995). Regionally, the onset of drier late Holocene conditions at Rantin Lake corresponds with the *Tiedemann-Peyto* advances (~3,700–2,600 cal yr BP) of alpine glaciers in northwestern North America (Clague et al. 2009; Koch et al. 2007; Osborn et al. 2007).

Conclusions

Interbedded sand layers, overturned bedding and ancient radiocarbon dates from the deep-water core (Core A-06) suggest that Rantin Lake levels were lower on average during the late glacial and early Holocene. Low calcium-carbonate concentrations and fine-grain sedimentation mark the transition to higher P/E at ~10,500 cal yr BP following a pronounced lowstand at ~10,700 cal yr BP. Increasing carbonate concentrations in Core A-06 by ~9,500 cal yr BP suggest decreasing water levels and drier conditions that intensified from ~9,500 to 8,400 cal yr BP. Littoral facies gradually transitioned to a mineral-rich facies by 8,400 cal yr BP, indicating the influx of shoreline sediments during the lowest lake levels of the sediment record. Fine-grained organic-rich sediment deposited from ~8,200 to 3,100 cal yr BP suggests that lake levels were higher during the middle Holocene. In general, the increasing trend in calcium-carbonate concentrations following minimum values at ~6,300 cal yr BP suggests that lake levels decreased slowly during the mid-Holocene until the end of the record at ~3,100 cal yr BP. In summary, the Rantin Lake water-level reconstruction provides evidence for higher P/E from ~10,500 to 9,500 cal yr BP, reduced P/E from ~9,500 to 8,400 cal yr BP and a transition to relatively wetter conditions between ~8,200 and 6,300 cal yr BP. Comparatively higher, yet decreasing water-levels were maintained from ~6,300 cal yr BP until the end of the record at ~3,100 cal yr BP.

Acknowledgments We thank Lindsey Watthaus, Bryan Friedman, Jordan Abbott and Lesleigh Anderson for their work in the field. We also thank Matthew Finkenbinder for his help with R and CLAM software, Kaitlin Clark for her work on XRD analysis and Ellen Fehrs for the loss-on-ignition analyses of Core A-06. Finally, we thank the National Science Foundation (ARCSS 0908200) and the University of Pittsburgh for supporting this research. This manuscript was greatly improved by the helpful suggestions from three anonymous reviewers.

References

Abbott MB, Strafford TW (1996) Radiocarbon geochemistry of ancient and modern lakes, Arctic lakes, Baffin Island. Quat Res 45:300–311

Abbott MB, Finney BP, Edwards ME, Kelts KE (2000) Lake-level reconstructions and paleohydrology of Birch Lake, central Alaska, based on seismic reflection profiles and core transects. Quat Res 53:154–166

Anderson L, Abbott MB, Finney BP, Edwards ME (2005) Palaeohydrology of the southwest Yukon Territory, Canada, based on multiproxy analyses of lake sediment cores from a depth transect. The Holocene 15:1172–1183

Benson L, White LD, Rye R (1996) Carbonate deposition, Pyramid Lake Subbasin, Nevada: 4. Comparison of the stable isotope values of carbonate deposits (tufas) and the Lahontan lake-level record. Palaeogeogr Palaeoclimatol Palaeoecol 122:45–76

Blaauw M (2010) Methods and code for 'classical' age-modelling of radiocarbon sequences. Quat Geochron 5:512–518

Bryson RA, Hare KF (1974) Climate of North America. In: Landsberg HE (ed) World survey of climatology. Elsevier, Amsterdam, pp 5–12

Clague JJ, Menounos B, Osborn G, Luckman BH, Koch J (2009) Nomenclature and resolution in Holocene glacial chronologies. Quat Sci Rev 28:2231–2238

Croudace IW, Rindby A, Rothwell RG (2006) ITRAX: description and evaluation of a new multi-function X-ray core scanner. In: New techniques in sediment core analysis. Geological Society Special Publications, London, pp 51–63

Cwynar LC, Spear RW (1995) Paleovegetation and paleoclimatic changes in the Yukon at 6 ka BP. Geogr Phys Quat 49:29–35

Dean WE (1974) Determination of carbonate and organic matter in calcareous sediments and sedimentary rocks by loss on ignition: comparison with other methods. J Sed Petr 44:242–248

Dean WE (2006) Characterization of organic matter in lake sediments from Minnesota and Yellowstone National Park. In: Open File Report 2006-1053, US Geological Survey Report, Reston, Virginia, p 40

Doherty RA, Mougeot CM, vanRanden JA (1994) Geological processes and terrain hazards of Watson Lake 105A. Exploration and geological services division, Yukon Region, Indian and Northern Affairs, Whitehorse, Yukon, Canada

Environment Canada (2010) Canadian Climate Normals 1971-2000, Watson Lake A, 2011 Fredericton, New Brunswick, Canada

Heiri O, Lotter AF, Lemcke G (2001) Loss on ignition as a method for estimating organic and carbonate content in sediments: reproducibility and comparability of results. J Paleolimnol 25:101–110

Kelts KE, Hsü KJ (1978) Freshwater carbonate sedimentation. In: Lakes AL (ed) Chemistry, geology, and physics. Springer, New York, pp 295–323

Koch J, Osborn GD, Clague JJ (2007) Pre-'Little Ice Age' glacier fluctuations in Garibaldi Provincial Park, Coast Mountains, British Columbia, Canada. The Holocene 17:1069–1078

Leng M, Marshall JD (2004) Palaeoclimate interpretation of stable isotope data from lake sediment archives. Quat Sci Rev 23:811–831

Lipovsky PS, McKenna K, Huscroft CA (2005) Surficial geology of Watson Lake (NTS 105A/2), Yukon (1:50,000). Yukon Geological Survey, Energy, Mines, and Resources, Yukon Government, Open File 2005–7

Mock CJ, Bartlein PJ, Anderson PA (1998) Atmospheric circulation patterns and spatial climatic variations in Beringia. Int J Clim 10:1085–1104

Osborn G, Menounos B, Koch J, Clague JJ, Vallis V (2007) Multi-proxy record of Holocene glacial history of the spearhead and Fitzsimmons ranges, southern British Columbia. Quat Sci Rev 26:479–493

Sanford WE, Wood WW (1991) Brine evolution and mineral deposition in hydrologically open evaporite basins. Am J Sci 291:687–710

Shapley MD, Ito E, Donovan JJ (2005) Authigenic calcium carbonate flux in groundwater-controlled lakes: implications for lacustrine paleoclimate records. Geochim Cosmochim Acta 69:2517–2533

Streten NA (1974) Some features of the summer climate of interior Alaska. Arctic 27:272–286

Stuiver M, Reimer PJ, Bard E, Beck JW, Burr GS, Hughen KA, Kromer B, McCormac FG, vd Plicht J, Spurk M (1998) INTCAL98 Radiocarbon age calibration 24,000–0 cal BP. Radiocarbon 35:215–230

Stuiver M, Reimer PJ, Reimer R (2010) CALIB Radiocarbon Calibration INCAL09 dataset. http://calib.qub.ac.uk/calib/

Teller JT, Last WM (1990) Paleohydrological indicators in playas and salt lakes, with examples from Canada, Australia, and Africa. Palaeogeogr, Palaeoclim Palaeoecol 76:215–240

Thompson JB, Shultze-Lam S, Beveridge TJ, Des Marais DJ (1997) Whiting events: biogenic origin due to the photosynthetic activity of cyanobacterial picoplankton. Limnol Oceanogr 42:133–141

Wahl HE, Fraser DB, Harvey RC, Maxwell JB (1987) Climate of the Yukon, Ottawa: Climatic Studies. Environment Canada, Atmospheric Environment Service, pp 1–323

Wright HE, Mann DH, Glaser PH (1984) Piston corers for peat and lake sediments. Ecology 65:657–659

Yu Z, Walker KN, Evenson EB, Hajdas I (2008) Lateglacial and early Holocene climate oscillations in the Matanuska Valley, south-central Alaska. Quat Sci Rev 27:148–161